

## 1.Detailed Justification for the Selection of the Equivalent Circuit

### Model for Fig 3 EIS Data

To clarify the rationale for selecting the equivalent circuit model for the electrochemical impedance spectroscopy (EIS) data presented in Figure 3 of the main text, this supplementary material systematically demonstrates the necessity of adopting the  $(R(CR)(L_R))$  model (i.e.,  $(R_S(CPER_F)(L R_L))$ ) from three perspectives: analysis of experimental spectrum characteristics, correspondence between the model and electrochemical processes, and validity of fitting parameters.

#### (1) Analysis of Experimental Spectral Characteristics

The Nyquist plot in Figure 3 of the main text shows a distinct inductive reactance feature (characterized by distortion or bulging of the capacitive arc) in the mid-frequency range after the addition of OPP400, which is particularly prominent at moderate concentrations (e.g., 4–40 mg/L). Meanwhile, the Bode phase angle plot exhibits a broadened single peak, indicating the coexistence of two interrelated relaxation processes at the corrosion interface.

A simple "capacitive arc" model (i.e., two series-connected CPE- $R_F$  parallel units) fails to characterize the inductive impedance characteristics in the mid-frequency range. Forcing a double capacitive arc model to fit the data while ignoring this inductive feature will result in systematic deviations between the simulated curves and experimental data across the corresponding frequency range. Therefore, it is imperative to incorporate a circuit component capable of describing this dynamic relaxation process into the equivalent circuit model.

#### (2) Correspondence Between Model and Electrochemical Mechanism

The selected  $(R(CR)(L_R))$  model (its structural diagram is presented in Figure 3g of the main text) provides a reasonable interpretation of the interfacial processes of magnesium in NaCl solutions containing adsorbed corrosion inhibitors, with each component assigned a clear physical meaning as follows:

$R_S$ : Represents the series solution resistance. Its value range (approximately 5–16  $\Omega \cdot \text{cm}^2$ ) is consistent with the conductivity of the 3.5 wt.% NaCl electrolyte employed in the experiments.

$CPE-R_F$ : This parallel component describes the high-frequency impedance response, which corresponds to the adsorbed protective film formed by OPP400 molecules on the magnesium surface. CPE characterizes the non-ideal capacitive behavior caused by microscopic inhomogeneities within the adsorbed film;  $R_F$  denotes the film resistance, which directly reflects the capacity of the adsorbed layer to impede ion migration. Notably, the value of  $R_F$  increases significantly with the rise of OPP400 concentration, which is consistent with the enhanced corrosion inhibition performance of the system.

$L_R$ : This parallel branch is dedicated to characterizing the inductive reactance observed in the mid-frequency range. For highly reactive metals such as magnesium, the mid-frequency inductive reactance in corrosion-inhibited media is typically associated with the relaxation of surface-adsorbed intermediate species (e.g.,  $Mg_{ads}^+$ )

or the dynamic process of metastable pitting initiation and repassivation. The introduction of this inductive branch enables the model to accurately reproduce both the inductive arc in the experimental Nyquist plots and the corresponding peak-broadening features in the Bode phase angle plots.

### (3) Validation of Model Fitting Rationality and Self-Consistency

- Fitting Quality and Spectral Reproducibility

When this model is applied to fit EIS data across all OPP400 concentrations, the simulated curves (solid lines in Figure 3 of the main text) show high concordance with the experimental data points over the entire frequency range ( $10^5$ – $10^1$  Hz), especially in the mid-frequency inductive reactance region. This demonstrates the model's excellent accuracy in describing the experimental electrochemical phenomena.

- Physical Significance and Variation Trends of Fitting Parameters

All fitted circuit parameters possess clear physical significance, and their variation patterns are fully consistent with the actual state of the corrosion system:

$R_F$  increases monotonically with the increase of OPP400 concentration, indicating the continuous strengthening of the protective adsorption film on the magnesium surface.

The exponent  $n$  of CPE increases from a relatively low value (~0.78) in the blank sample to a high value (~0.92) at the optimal OPP400 concentration, which reflects the transition of the electrode/electrolyte interface from a rough, non-uniform state to a smooth, uniform and integral adsorption film state.

The parameters of the inductive branch ( $L$ ,  $R_L$ ) are prominent at moderate OPP400 concentrations; whereas at high concentrations (100 mg/L), the inductive arc contracts and  $R_L$  increases, indicating a tendency toward complete surface coverage by OPP400 molecules, accompanied by the reduction of dynamic adsorption/desorption processes or local surface activation events.

- Cross-Validation with Independent Experimental Results and Literature

The variation trend of the total polarization resistance ( $R_P$ ) derived from this equivalent circuit model is in perfect agreement with the trend of corrosion current density ( $i_{corr}$ ) measured from potentiodynamic polarization curves, both of which indicate the same corrosion inhibition efficiency trend of OPP400.

This model has been widely adopted and validated in relevant research on the corrosion and inhibition of magnesium and magnesium alloys, with sufficient literature support confirming its applicability in describing metal corrosion systems containing organic adsorption layers.

In summary, based on the distinct inductive impedance characteristics observed in the mid-frequency range of the experimental EIS spectra, the dynamic electrochemical processes at the magnesium corrosion interface corresponding to this inductive feature, and the excellent fitting capability and parameter consistency exhibited by the  $R_S(CPE_R_F)(L R_L)$  model, we conclude that this equivalent circuit model is the most reasonable choice for analyzing the EIS data of the present system. It ensures the reliability of the subsequently extracted key electrochemical parameters (e.g.,  $R_F$ ,  $n$ ,  $R_P$ ), laying a solid foundation for elucidating the corrosion inhibition mechanism of OPP400.

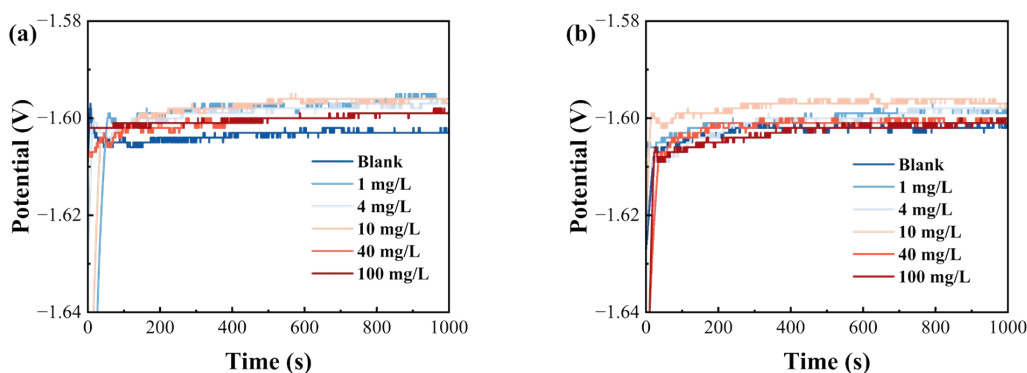
## 2. OCP Analysis

Changes in OCP act as a crucial indicator for characterizing electrode surface conditions and corrosion behavior. S. 1 presents the OCP evolution curves of pure Mg and Mg alloy when immersed for 1000 s in 3.5 wt.% NaCl solutions with different concentrations of OPP400.

For the pure Mg system, the initial OCP of the blank group was  $\sim$ 1.608 V. Subsequently, it gradually shifted positively with fluctuations, eventually stabilizing at  $\sim$ 1.603 V. These sustained fluctuations reflect the dynamic corrosion process involving the formation and detachment of surface corrosion products. Following the addition of OPP400, the OCP exhibited significant changes: all inhibitor-containing systems showed positive potential shift, with markedly reduced fluctuation amplitude. For instance, at 100 mg/L OPP400, the OCP rapidly shifted positively to  $\sim$ 1.597 V ( $\sim$ 5 mV higher than that of the blank group) and stabilized after 300 s, with fluctuations of less than 10 mV. This indicates that OPP400 molecules rapidly adsorbed to form a stable film, effectively suppressing localized corrosion reactions on the Mg surface.

Mg alloy also exhibit similar trends, but their overall OCP is higher than that of pure Mg. The steady-state potential of the blank group was  $\sim$ 1.602 V, which is attributed to the presence of a natural oxide film on their surfaces and the inhibitory effect of alloying elements. After adding 100 mg/L OPP400, the OCP of the Mg alloy shifted positively to  $\sim$ 1.600 V, with positive shift of  $\sim$ 2 mV. This further confirms the effective coverage and stabilizing effect of the inhibitor film on the alloy surface.

According to electrochemical corrosion theory, if the change in corrosion potential ( $E_{corr}$ ) following the addition of a corrosion inhibitor is less than 85 mV, the inhibitor can be classified as a mixed-type corrosion inhibitor. The observed positive shifts in OCP in this study were all significantly below this threshold, indicating that OPP400 simultaneously inhibits both the anodic dissolution reaction ( $Mg \rightarrow Mg^{2+} + 2e^-$ ) and the cathodic hydrogen evolution reaction ( $2H_2O + 2e^- \rightarrow H_2 + 2OH^-$ ). This conclusion is consistent with the results of subsequent PDP tests.

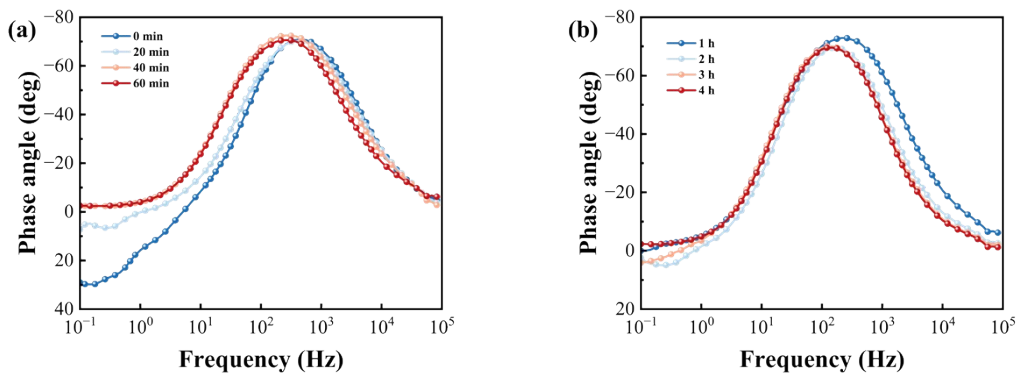


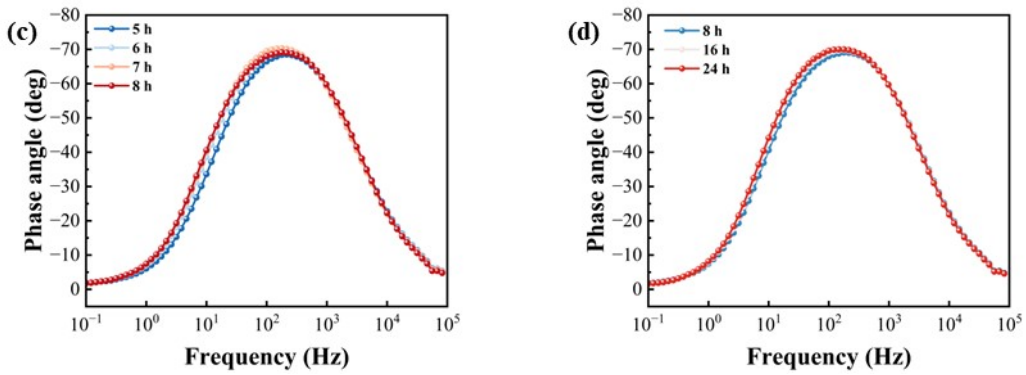
S. 1 OCP evolution curves of (a) pure Mg and (b) Mg alloy in 3.5 wt.% NaCl solutions with different OPP400 concentrations

### 3. The Evolution Process of Corrosion Products

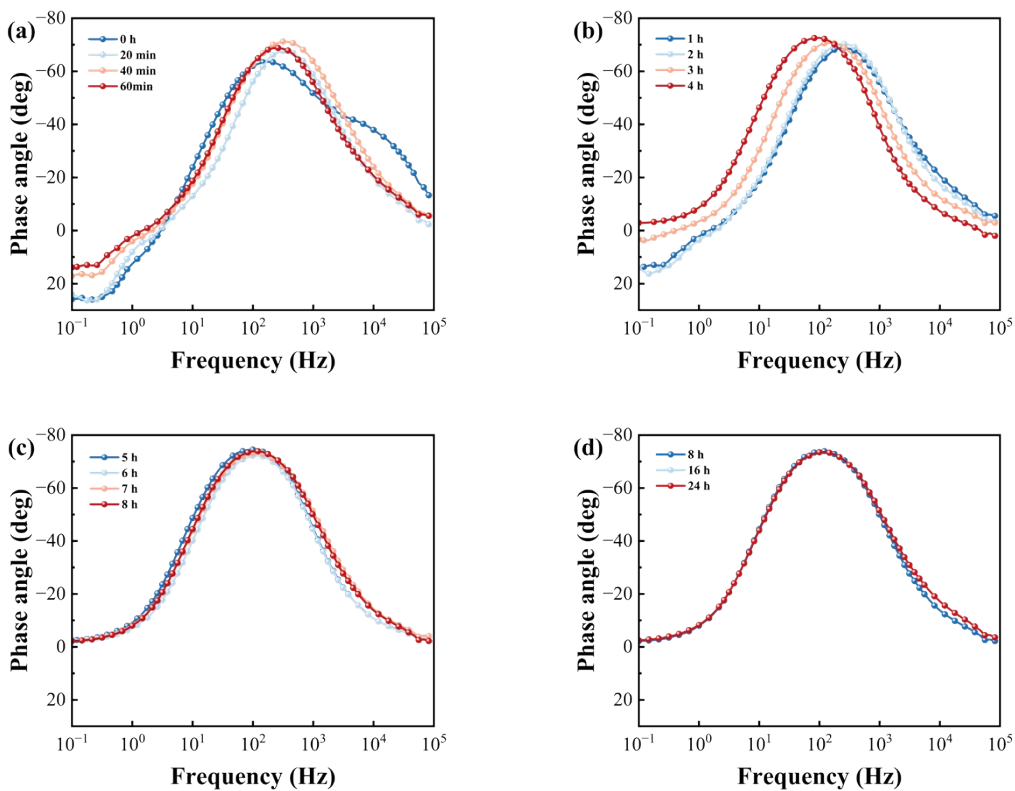
This study systematically analyzed the phase angle-frequency responses of Bode plots for pure Mg and AZ Mg alloy in 3.5 wt.% NaCl solutions with and without the OPP400 corrosion inhibitor (S. 2-5), which reveals the dynamic evolution mechanism of interfacial corrosion and corrosion inhibition processes. As key parameters in EIS, the evolution of the phase angle peaks and characteristic frequencies reflects the formation processes of the interfacial double-layer structure, corrosion product deposition, and inhibitor adsorption film—providing crucial insights into the corrosion kinetics of Mg and Mg alloy.

For pure Mg systems, the evolution of the phase angle is directly related to the deposition and stabilization of the surface  $\text{Mg}(\text{OH})_2$  layer. In the NaCl solution (S. 2), during the initial immersion period (0–60 min), the phase angle peak gradually increases while the characteristic frequency shifts to lower frequencies. This indicates continuous accumulation of corrosion products, with the interfacial capacitance behavior gradually transitioning from double-layer-dominated to corrosion product film-dominated. After approximately 2 hours, the curves converge and the parameters stabilize, signifying a dynamic equilibrium between the accumulation and dissolution of the product layer. However, this layer remains loose and porous, which is unable to effectively block  $\text{Cl}^-$  penetration. In the solution containing 100 mg/L OPP400 (S. 3), the corrosion inhibitor promotes the formation of a dense “ $\text{Mg}(\text{OH})_2$ –OPP400 composite film” through a synergistic mechanism involving chelation of  $\text{Mg}^{2+}$  by phosphate groups and hydrophobic blocking by oleic acid chains. This process is reflected in the continuous rise of the phase angle peak and the steady decrease in the characteristic frequency, and reaches stability after approximately 4 hours. This indicates that the interfacial state enters a long-term stable phase after inhibitor molecular adsorption and film layer reorganization, consistent with the Langmuir monolayer adsorption mechanism.





S. 2 Phase angle-frequency curves of pure Mg immersed in 3.5 wt.% NaCl solution at different immersion times

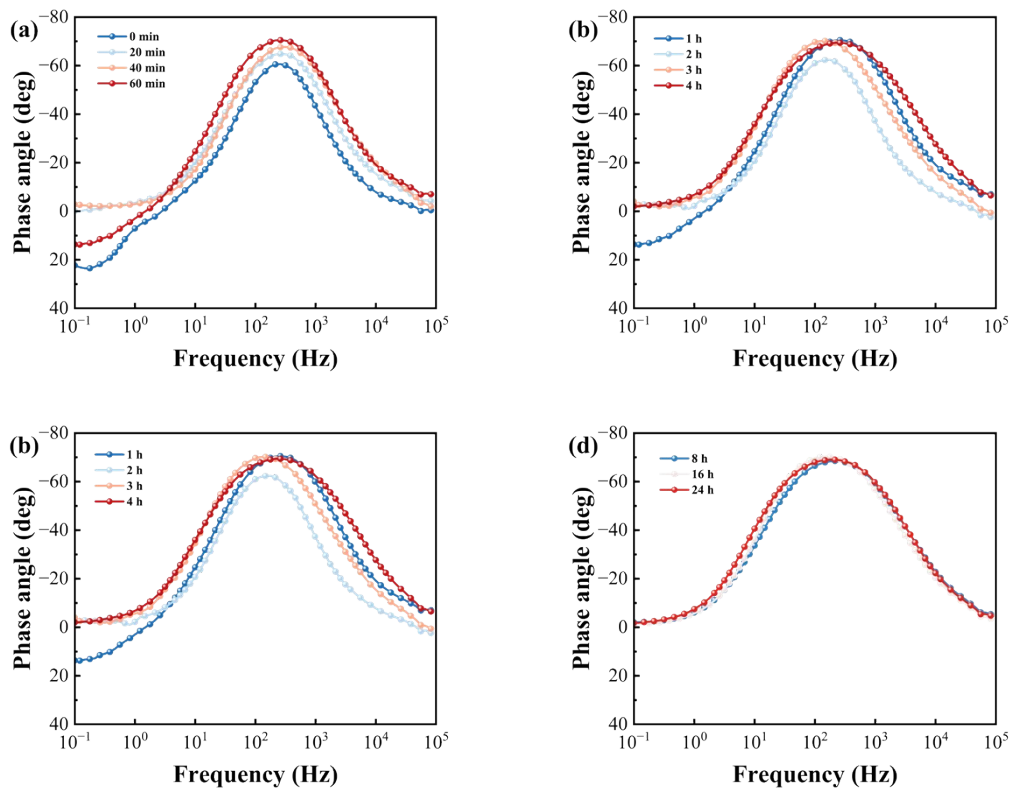


S. 3 Phase angle-frequency curves of pure Mg immersed in 3.5 wt.% NaCl solution containing 100 mg/L OPP400 at different immersion times

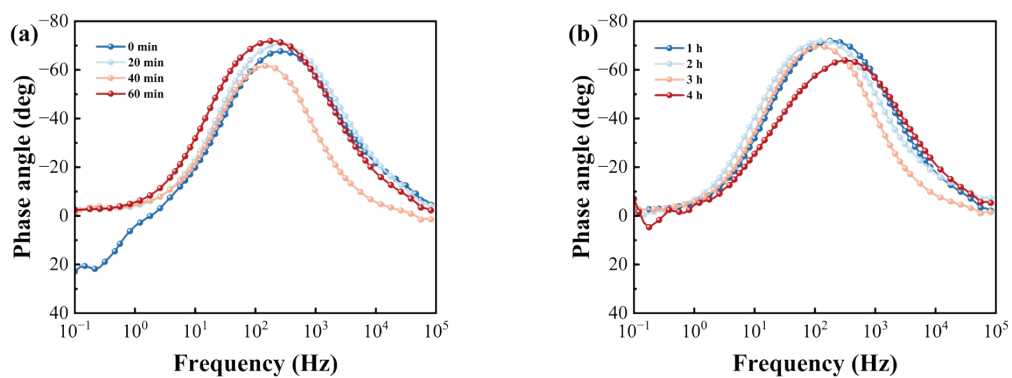
The presence of trace amounts of the  $\beta$ -  $Mg_{17}Al_{12}$  phase in AZ-series Mg alloy significantly influences their interfacial evolution pathways (S. 4 and S. 5). In the OPP400-containing system, the  $\beta$  phase acts as active sites, preferentially adsorbing OPP400 molecules and promoting  $Mg(OH)_2$  deposition. This shortens the phase angle stabilization time compared to that of pure Mg, indicating accelerated composite film formation. Simultaneously, the curves exhibit a high degree of overlap between 4 and 24 hours, demonstrating excellent film stability and indicating that the  $\beta$  phase enhances film-substrate adhesion. In contrast, in the blank solution, the microgalvanic effect causes an uneven distribution of the electrochemical state at the interface. The phase angle-frequency curves exhibit broadening or even multiple relaxation characteristics,

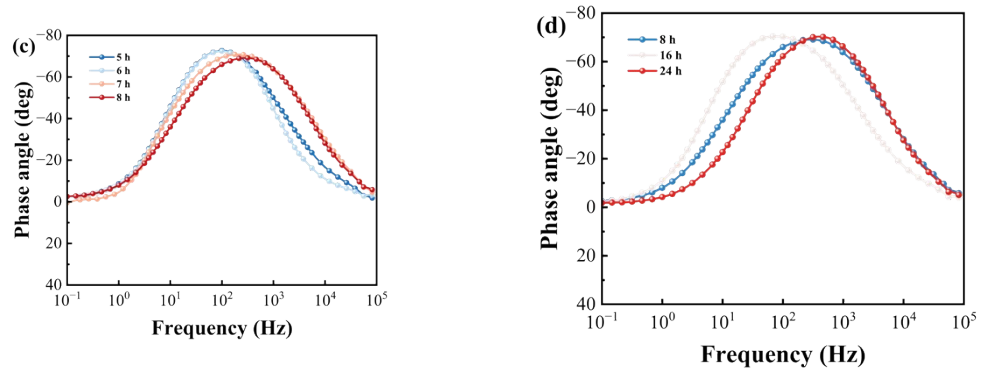
indicating significant differences in corrosion behavior between the  $\alpha$ -Mg matrix and  $\beta$  phase, with localized corrosion being more pronounced.

This study established a phase angle parameter-based evaluation framework for interfacial corrosion processes in Mg alloy: the peak phase angle rise rate reflects the densification efficiency of the interfacial film; the characteristic frequency shift characterizes the transition of relaxation mechanisms; and the overlap and stability of the curve family represent the film's uniformity and long-term protective capability. OPP400 promotes the formation of a highly stable composite film through a synergistic adsorption mechanism, effectively retarding the interfacial corrosion process. The  $\beta$  phase in Mg alloy plays a dual role in both “induced deposition” and “microgalvanic corrosion.”



S. 4 Phase angle-frequency curves of Mg alloy in 3.5 wt.% NaCl solution at different immersion times





S. 5 Phase angle-frequency curves of Mg alloy immersed in 3.5 wt.% NaCl solution containing 100 mg/L OPP400 at different immersion times